

Studies on current-voltage, capacitance-voltage and optical illumination effect in MISIM nanostructure devices

Soumen Banerjee, Subhajit Mukherjee, Tuhin Das, Abhishek Barik

Department of Electronics & Communication Engineering
Hooghly Engineering and Technology College, Pipulpati, Hooghly, West Bengal, India

ABSTRACT : A quantum mechanical model of MISIM structure has been considered and its current-voltage characteristics has been studied for different insulator thickness, inter-electrode separation and device temperature before and after inversion both in presence and absence of oxide trap levels. The current-voltage characteristics exhibit an S-type NDR after threshold inversion voltage which depends on oxide thickness and other parameters. The capacitance-voltage has also been studied along with the current-voltage characteristics under optical illumination. The results obtained are found to be in close conformity with the theory of tunneling effect.

Keywords: MISIM diode, Negative Differential Resistance, Tunneling effect, WKB Approximation.

I. INTRODUCTION

Metal-Insulator-Semiconductor (MIS) devices with ultrathin oxide layers where novel quantum effects rise owing to tunneling wave have been reported in literature in recent years. Metal-Insulator-Semiconductor-Insulator-Metal (MISIM) devices exhibiting quantum tunneling has also been recently reported [1-2]. MISIM structure is of interest to researchers worldwide owing to its applications in several domains as reported in literature [3-6]. Based on the model of MIS tunnel diode, a simple model of MISIM structure has been proposed considering the semiconductor as n-type Silicon with insulating layer as an ultrathin (1-3 nm) layer of silicon dioxide and metal being aluminum. The tunneling current has been evaluated by considering the nanostructure comprising of different layers. The supply function considers Fowler-Nordheim electron emission scheme [7] from the metal and WKB approximation has been used to obtain the electron wave function in different regions. The current-voltage (I-V) characteristic is obtained considering tunneling components of current from different layers of MISIM structure. The effect of oxide thickness, temperature and inter-electrode distance on the I-V characteristics is studied along with current multiplication mechanism of MISIM device. The capacitance-voltage (C-V) characteristic is also studied. The device is found to exhibit an S-type Negative Differential Resistance (NDR) thereby revealing the potentiality of generating high output power at high frequency. A study of applied voltage versus device current has also been carried out with and without optical illumination effect in MISIM nanostructure device.

II. DESIGN METHODOLOGY

The potential profile of MISIM diode as depicted in Fig. 1 has been obtained from the solution of 1-D Poisson's equation. The potential profile is shown by the continuous line while the horizontal broken line depicted in Fig. 1 represents a single value of total electron energy E_x , which is assumed to be constant throughout the device structure.

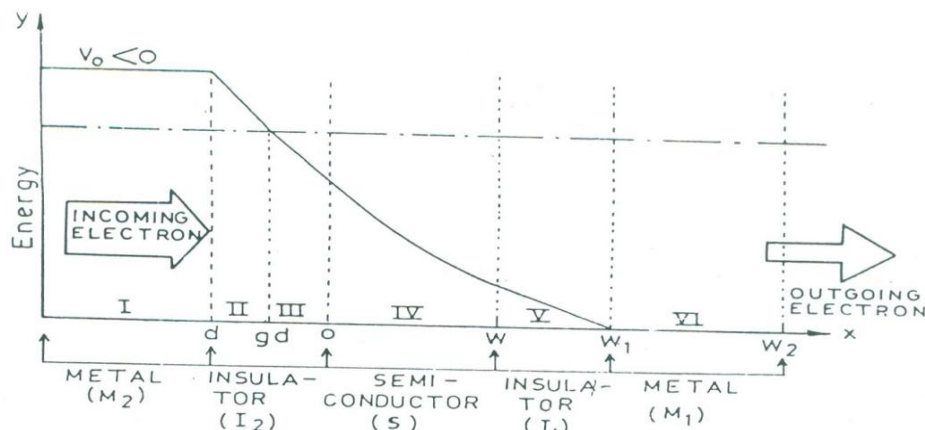


Fig. 1. MISIM Nanostructure Device

The potential functions for different regions are expressed by the following equations:

$$\begin{aligned}
 V = V_0 &= \text{The negative applied voltage} && \text{in the region } x < -d \text{ (Region I)} \\
 V = D - Ex & && \text{in the region } -d \leq x < 0 \text{ (Regions II \& III)} \\
 V = -Ax^2 + Bx + C & && \text{in the region } 0 \leq x < W \text{ (Region IV)} \\
 V = V_1 - \frac{V_1(x-W)}{(W_1-W)} = V_1 - \frac{V_1(x-W)}{d} & && \text{in the region } W \leq x < W_1 \text{ (Region V)} \\
 V = 0 &= \text{datum level of voltage} && \text{in the region } W_1 \leq x < W_2 \text{ (Region VI)} \\
 \dots & (1)
 \end{aligned}$$

where, $D = V_0 - \frac{|Q_s|}{\epsilon_i}d$, $E = \frac{|Q_s|}{\epsilon_i}$, Q_s = Surface charge density at the semiconductor, ϵ_i = permittivity of

the insulator, d = insulator thickness, V_1 = potential at $x=W$, $A = \frac{\tilde{E}}{2W}$, $B = \tilde{E}$, $C = V_s = \frac{qN_D W^2}{2\epsilon_s}$,

\tilde{E} = electric field at $x=0$, N_D = donor concentration and ϵ_s = permittivity of the semiconductor.

WKB approximation is used to obtain the electron wave functions of the MISIM structure which is divided into six regions from I to VI as depicted in Fig. 1. The effective mass of electron in metal, insulator and semiconductor are taken to be m_m^* , m_i^* and m_s^* respectively. The electron wave function in different regions is obtained as

$$\Psi_1 = a_1 \exp(k_1 x) + a_2 \exp(-k_1 x). \quad \dots (2)$$

$$\Psi_2 = b_1 \frac{(2m_i^*)^{-1/4}}{\eta^{-1/2}} (\alpha - \beta x)^{-1/4} \exp \left\{ -\frac{2}{3} \frac{\sqrt{2m_i^*}}{\eta\beta} (\alpha - \beta x)^{3/2} \right\} \quad \dots (3)$$

$$\Psi_3 = c_1 \frac{(2m_s^*)^{-1/4}}{\eta^{-1/2}} (\alpha' - \beta' x)^{-1/4} \exp \left\{ i \frac{2}{3} \frac{\sqrt{2m_s^*}}{\eta\beta'} (\alpha' - \beta' x)^{3/2} \right\} \quad \dots (4)$$

$$\Psi_4 = d_1 H^{-1/2} (x - W)^{-1/2} \exp \left\{ \frac{i}{2} H (x - W)^2 \right\} \quad \dots (5)$$

$$\Psi_5 = e_1 \frac{(2m_i^*)^{-1/4}}{\eta^{-1/2}} \exp \left\{ i \frac{2}{3} \frac{\sqrt{2m_i^*}}{\eta\beta_1} (\alpha_1 - \beta_1 y)^{3/2} \right\} \quad \dots (6) \quad \text{with } y = x - W$$

$$\Psi_6 = f_1 \exp(ik_1 x) \quad \dots (7)$$

where, $\psi_1, \psi_2, \dots, \psi_6$ are the electron wave-functions in the regions I, II, ... VI respectively and $a_1, a_2, b_1, c_1, d_1, e_1, f_1$ are arbitrary constants. E_x is measured in eV unit.

$$\begin{aligned}
 k_1 &= \frac{\sqrt{2m_m^* |V_0 - E_x|}}{\eta}, \quad \alpha = D - E_x = -\alpha', \quad \beta = E = -\beta', \quad H = \frac{\sqrt{2m_s^* A(1+r)}}{\eta}, \\
 r &= \frac{4}{W} \left\{ \frac{2(E_x - V_s)}{\tilde{E}} - 1 \right\}, \quad \alpha_1 = E_x - V_1, \quad \beta_1 = \frac{V_1}{(W_1 - W)} = \frac{V_1}{d}, \quad k_6 = \frac{\sqrt{2m_m^* E_x}}{\eta}
 \end{aligned}$$

The net tunneling probability of an electron with energy E_x is given by,

$$T(E_x) = \frac{m_i^*}{(m_m^*)^{3/2}} \frac{4k_1^2}{(A_1k_1 + A_2)^2} \frac{\eta}{\sqrt{2\epsilon_0}} \exp(-2k_1d) \quad \dots (8)$$

The current density in Fowler-Nordheim scheme is given by $J_{FN} = \int_{AllEnergies} qT(E)N(E)dE$

where $N(E_x)dE_x$ is given by $N(E_x)dE_x = \frac{4\pi m_m^* k_B T}{h^3} \ln \left\{ 1 + \exp \left(-\frac{E_x - \epsilon_F}{k_B T} \right) \right\} dE_x \quad \dots (9)$

Tunneling current from metal - A single energy level of electron having the value of E_x has been considered. At finite non-zero absolute temperature T , the Fermi-Dirac distribution exhibits a tail which implies that there are same electrons having energy greater than E_F by $K_B T$ as shown in Fig. 2 and Fig. 3.

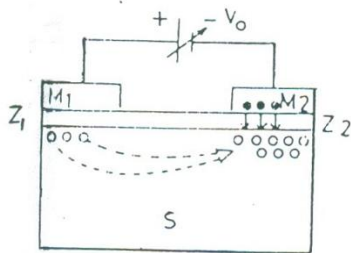


Fig. 2.

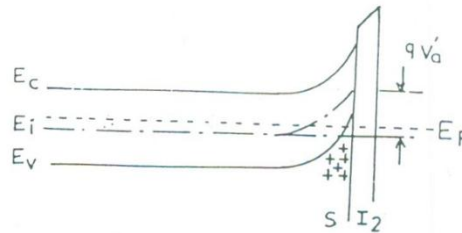


Fig. 3.

Electrons having total energy in the range $(E_F - K_B T) \leq E_x \leq E_F$ can absorb some energy from phonons and take part in tunneling. Tunneling for the electrons having total energy in the range $E_F \leq E_x \leq (E_F + K_B T)$ is easier. Therefore, tunneling current density due to electrons from metal M_2 is given by

$$J_t = q \int_{E_F - k_B T}^{E_F + k_B T} T(E_x) N(E_x) dE_x$$

Tunneling current from semiconductor and insulator - Using WKB approximation the tunneling current of a conduction band electron is given by

$$T_c(E) = \exp \left[-\frac{\sqrt{2m_i^*}}{\eta\sqrt{2}} (Wl)^{3/2} \int_0^2 \sqrt{\left| \left(x'' - \frac{2}{l} \right)^2 - R' \right|} dx'' \right] \quad \dots (10)$$

The tunnelling current density from the semiconductor is

$$J_c = \int_{E_c - k_B T}^{E_c + k_B T} qT_c(E) f(E) D_c(E) dE \quad \dots (11)$$

Trap levels E_{t1} & E_{t2} are assumed to be present at the insulators I_1 & I_2 respectively and the tunneling current from these levels are given by

$$J_{t1} = q \int_{E_c - k_B T}^{E_c + k_B T} T_{t1}(E) N_{t1}(E) dE \quad \dots (12)$$

$$J_{t2} = q \int_{E_F - k_B T}^{E_F + k_B T} T_{t2}(E) N_{t2}(E) dE$$

Hence, the total current density from the conduction band trap levels is therefore given by

$$J_{addl} = J_c + J_{t1} + J_{t2}$$

The I-V characteristic exhibits a Negative Differential Resistance (NDR) of S-type which is in conformity with the reported experimental results [2]. The current multiplication factor is expressed as

$$\gamma = \frac{I_0}{I_i} = \frac{I_h + I_i}{I_i} = 1 + \frac{I_h}{I_i} \quad \dots (13)$$

Capacitance in MISIM diode - The semiconductor in M_1I_1S side is forward biased. The capacitance that comes into play in this junction is Capacitance dependent on insulation properties and Diffusion Capacitance due to storage charge. The semiconductor in M_2I_2S side is reverse biased. The capacitance that comes into play in this junction is Depletion layer capacitance and Capacitance dependent on insulator properties. When no external bias is applied to the structure, there is a contact potential formed due to the work function difference of metal and semiconductor. This built-in potential Φ_{ms} across M_1S and $-\Phi_{ms}$ across M_2S will contribute in different capacitances. In region M_1I_1S , which is in accumulation mode, the junction

capacitance dependent on insulator properties is $C_i = \frac{\epsilon_i}{d}$

.... (14)

The diffusion capacitance has been found out to be $C_D \approx n_{n0} \frac{q^2}{k_B T} \exp\left\{\frac{q}{k_B T}(V_s - \phi_{ms})\right\}$ (15)

where, n_{n0} is the equilibrium concentration in the semiconductor. The net capacitance of the MISIM nanostructure is given by

$$C_{net} = \frac{C_{M_1I_1S} C_{M_2I_2S}}{C_{M_1I_1S} + C_{M_2I_2S}} = \frac{C_i C_D C_d}{C_d(C_i + C_D) + C_D(C_i + C_d)} \quad \dots (16)$$

Equation (16) can be used to obtain the C-V characteristics of the MISIM nanostructure device. As the thickness of the oxide layer is increased, the junction capacitance of the structure is decreased, which in turn, reduces the net capacitance of the structure. The rate if decrease of the net capacitance with oxide thickness d is given by

$$\frac{dC_{net}}{dd} = \frac{-C_j^2 C_D^2}{C_d(C_j + C_D) + C_D(C_j + C_d)} \left(\frac{\epsilon_i}{d^2}\right) \quad \dots (17)$$

III. RESULTS AND DISCUSSIONS

The I-V characteristics of MISIM diode has been studied varying oxide thickness, inter-electrode separation and temperature. Fig. 4 depicts the I-V characteristics at room temperature for different oxide thickness (d) keeping inter-electrode separation (W) constant. The plot reveals that the tunneling current increases with decrease in oxide thickness as the barrier width decreases in this case. Also the hole current increases with decrease in oxide thickness as the drop across the semiconductor region increases. Hence the total current increases with decrease in oxide thickness at a constant applied voltage. The I-V characteristics exhibits an S-type NDR when the applied voltage is sufficient to form inversion layer. Fig. 5 depicts the I-V characteristics for different inter-electrode separation. The inversion threshold voltage and the tunnel current do not depend upon inter-electrode separation (W). However, the total current decreases with increasing W after inversion. This is due to fall of hole component of current with increase of W . This is depicted in Fig. 5. Fig. 6 exhibits the I-V characteristics at three different temperatures keeping oxide thickness and inter-electrode separation constant. The tunneling current increases with temperature owing to its dependence on the supply function which in turn increases with temperature. The rate of increases of hole current with applied voltage after inversion decreases with increase in temperature but there is a cross-over after a certain applied voltage. This is because in this voltage region the tunneling current predominates over hole component of current. Fig.7 and Fig.8 depicts the plot of current multiplication factor with applied voltage and temperature (after inversion) respectively. The current multiplication factor decreases sharply with increase in temperature up to about $380^{\circ}C$ and the rate of fall decreases. It also decreases with applied voltage. Fig. 9 depicts a plot of capacitance-voltage characteristics for a MISIM nanostructure device with oxide thickness equal to 2 nm. Fig. 10 and Fig. 11 depict I-V characteristics of the device without and with illumination (1000 W bulb). When MIS structure is illuminated electron-hole pair is generated optically; thereby reducing the surface potential at silicon-insulator junction. This hinders the inversion process and hence the inversion threshold voltage becomes large. Hence, at comparatively low voltage region current is constituted only due to tunneling effect. The experimental nature of this current is in conformity with the theory of tunneling current.

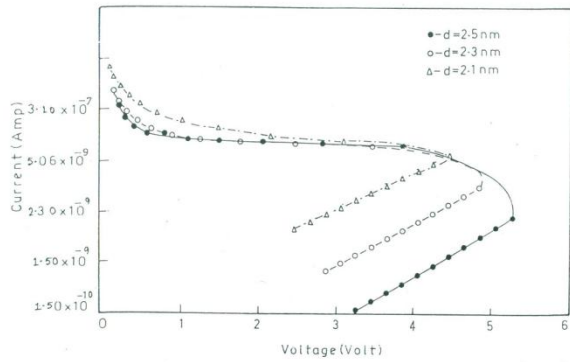


Fig. 4. Variation of current with voltage at room temperature for different oxide thickness (d)

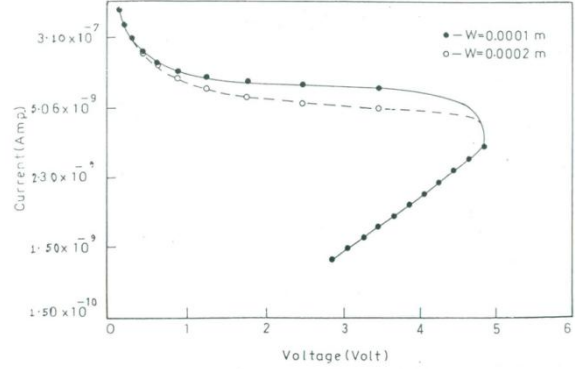


Fig. 5. Variation of current with voltage for different inter-electrode separation (W)

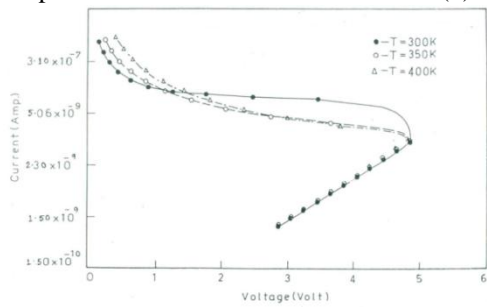


Fig. 6. Variation of current with voltage at different temperature (keeping oxide thickness and inter-electrode separation constant)

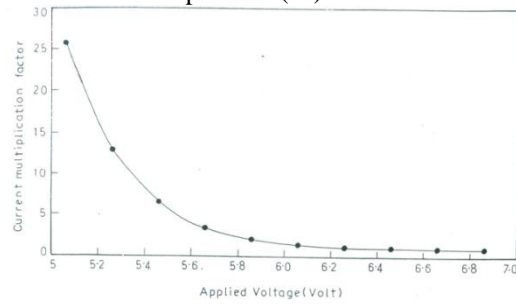


Fig. 7. Variation of current multiplication factor with applied voltage

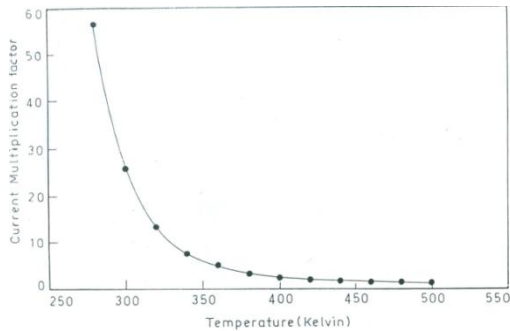


Fig. 8. Variation of current multiplication with temperature (after inversion)

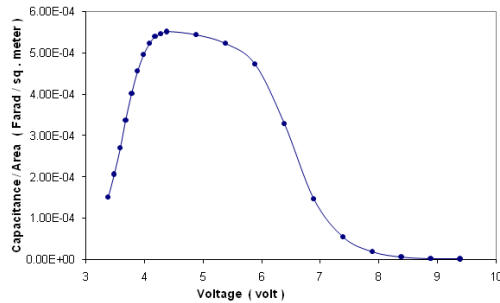


Fig. 9. Variation of capacitance with voltage with oxide thickness = 2 nm

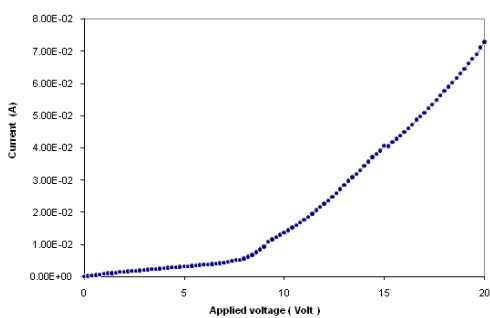


Fig. 10. Variation of current with applied voltage (without illumination)

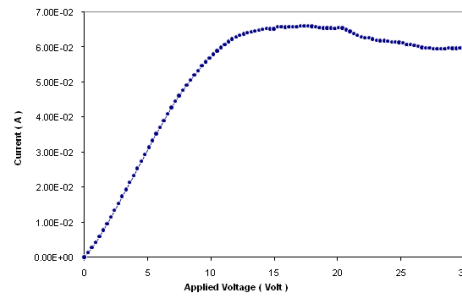


Fig. 11. Variation of current with applied voltage (with illumination of 1000 W)

IV. CONCLUSION

The present paper, considering a quantum mechanical model of MISIM Nanostructure diode, reveals that the characteristics of the device exhibits strong potentiality of the device to generate high frequency power. The results obtained will be very useful in designing of the device and its use as a low noise RF power generator in the millimeter wave region.

REFERENCES

- [1] T. P. Das, Soumen Banerjee and J. P. Banerjee, Quantum Mechanical Model of MISIM Nanostructures, Proc. XIth Int. Workshop on the Physics of Semiconductor Devices (IWPSD- 2001), 1, IIT Delhi, 2001, 338-342.
- [2] Bogdan Majkusiak, Experimental and theoretical study of the current - voltage characteristics of the MISIM tunnel transistor, IEEE Trans. ED, 45 (9), 1998, 1903-1911.
- [3] W. J. Wang et. al., MISIM Structured Titanium Dioxide Ultraviolet Photodetector, J. Phys. D: Appl. Phys., 43, 2010, 1-4.
- [4] W. C. Liu et. al., Multiple Negative-Differential resistance (MNDR) phenomena of a MISIM-like structure with step-compositioned $\text{In}_x\text{Ga}_{1-x}\text{As}$ quantum wells, IEEE Trans. ED, 45 (2), 1998, 373-379.
- [5] W. K. Chan et. al., High-speed $\text{Ga}_{0.47}\text{In}_{0.53}\text{As}$ MISIM photodetectors with dielectric-assisted Schottky barriers, IEEE Trans. ED Letters, 10 (9), 1989, 417-419.
- [6] M. Darwish and K. Board, Theory of switching in MISIM structures. IEE Proc., 128 (5), 1981, 165-173.
- [7] M. Rasras, I. De Wolf, G. Groeseneken, B. Kaczer, Robin Degraeve and H. E. Maes, Photocarrier generation as the origin of Fowler-Nordheim induced substrate hole current in thin oxides, IEEE Trans. ED, 48 (2), 2001, 231.